Roll-Bonded Tri-Layered Mg/Al/Stainless Steel Clad Composites and their Deformation and Fracture Behavior

IN-KYU KIM and SUN IG HONG

The deformation and fracture behaviors of roll-bonded tri-layered Mg/Al/stainless steel (SST) composite plates were studied. Brittle interfacial reaction compounds were observed at the Mg/Al interface upon annealing at and above 573 K (300 °C), whereas no visible interfacial reaction compounds were observed at Al/SST interfaces even after annealing up to 673 K (400 °C). The strength of the tri-layered Mg/Al/SST clad plates is in close agreement with those calculated from the strength data of the separated Mg, Al, and ST layers using the rule of mixture. The fracture strain components of the tri-layered clad in the absence of brittle interfacial intermetallic layer far exceed those calculated based on the fracture strain data of separated Mg, Al, and SST sheets. The enhanced ductility of the clad composites is due to the suppression of the localized deformation in a metallic layer by other metallic layers caused by the mutual constraint imposed by an adjacent layer. On the other hand, the fracture strain was found to be reduced in the presence of intermetallic layers between the metallic substrates. Cracks perpendicular to the stress axis were observed in the intermetallic compound layer between Mg and Al, inducing the localized slip in the vicinity of intermetallic cracks and premature fracture of the Mg alloy layer.

DOI: 10.1007/s11661-013-1697-8

I. INTRODUCTION

THERE has been a continued interest in lighter-weight materials to enhance the fuel efficiency in the automobile industry, and research on Mg alloy focusing on mechanical properties has become very active in the last decade.[1–7] The application of Mg and its alloys is still limited because they have crucial drawbacks, such as poor corrosion resistance, poor formability, and high cost, compared to Al and its alloys, despite extensive research and development on magnesium and its alloys.[1–7] The most serious impediment to the application of Mg alloys is its intrinsic poor corrosion resistance.[7] The challenge to improve the corrosion resistance by alloying has had no satisfactory results, probably because of its intrinsic nature of non-protective oxide films.

Cladding Mg with Al and Al alloys was found to be an effective way to protect Mg alloys and improve the poor corrosion resistance[7] because Al alloys with a protective surface Al_2O_3 oxide layer can protect Mg against oxidation and corrosion. Stainless steel (SST) also has corrosion resistance and excellent mechanical strength.[8] Despite many attractive properties of stainless steels (SST), higher density limited the more general application of SST to vehicle parts and auto bodies. Cladding Mg with thin stainless steel (SST) may be considered as a viable option since it can provide the optimum combination of excellent corrosion resistance and the strength of SST and the low weight of Mg. However, studies on Mg/steel cladding are scarce.[8] Cetin *et al.*[8] showed that steel-magnesium alloy laminated metal composites (LMCs) produced by gas pressure infiltration of a liquid magnesium alloy between layers of stacked steel sheets are nearly as ductile as the steel, implying that the magnesium alloy in the as-cast LMCs has a substantially increased tensile ductility. Similarly, steel clad Mg, like Al clad Mg,[9,10] may have many desirable properties such as excellent corrosion resistance and formability which can be exploited in a wide range of structural applications. Cladding Mg alloys to stainless steels can reduce the density of the material and still exploit the excellent corrosion resistance of stainless steels.

Solid state cladding of Mg and SST by mechanical joining through rolling at low and intermediate temperatures is difficult because of the limited deformability of Mg due to limited slip systems and high strength of SST. Al may be used as a good interlayer metal between Mg and SST[11] since it was proven to be joined to both SST[9,10] and Mg[11,12] because of its excellent deformability at low and intermediate temperatures. The roll bonding method is currently the most common process for producing clad sheets because of its efficiency and cost competitiveness compared to other processing methods. Recently, Kim *et al.*[12] worked on cladding Mg/Al/SST with relatively thick Al and SST layers (Mg: 1.6 mm; Al: 1.2 mm; SST: 1 mm) and published their preliminary results. In this work, thicker Mg alloy sheets (2.3 mm) clad with a thinner SST 430 sheet (0.5 mm) with a thinner 3004 Al alloy interlayer (1 mm) were fabricated by a roll bonding process and the mechanical

IN-KYU KIM, Graduate Student, and SUN IG HONG, Professor, are with the Department of Nanomaterials Engineering, Chungnam National University, Daejeon 305-764, South Korea. Contact e-mail: sihong@cnu.ac.kr

Manuscript submitted November 1, 2012.
Article published online March 20, 2013

responses and fracture behaviors were studied. The interfacial reaction products after annealing and its effect on the mechanical properties of the roll-bonded AZ31 Mg/3004 Al/18 pct Cr ferritic stainless steel (SST 430) clad plates were also studied. The objective of this research is to examine the mechanical properties of annealed clad metals in relation to the interfacial properties.

II. EXPERIMENTAL

A tri-layered Mg/Al/SST composite was fabricated by the roll bonding process. Mg(AZ31), Al(Al 3004), and SST(SST430) sheets with the initial thickness of 5 mm, 1.8, and 0.7 mm, respectively, were stacked after degreasing and scratch brushing and hot-roll-bonded at 573 K (300 °C) with the reduction ratio of 49.3 pct. The Mg/Al/SST clad metal plate after roll bonding has a total thickness of 3.8 mm and that of the Mg, Al ,and SST sheet was 2.3 mm, 1, and 0.5 mm, respectively (Figure 1). The Al(Al 3004) sheet was inserted between the Mg(AZ31) sheet and the SST(SST 430) sheet to enhance the bonding between SST and Mg. Table I shows the chemical composition of the material sheets used in this study. The roll-bonded clad Mg/Al/SST plate was heat treated at various temperatures [473 K, 573 K, 673 K (200 °C, 300 °C, 400 °C) for 1 hour and 673 K (400 °C) for 3 hours] to examine the interfacial reaction of Mg/Al and Al/SST interfaces. To examine the interfacial properties, the tensile test were performed at room temperature using a Universal Materials Testing Machine (UNITED, US/SSTM). Tensile specimens with a gage length of 15 mm and the gage width of 3.4 mm were mechanical tested at an initial strain rate of $1\times10-3/s$. To examine the variation of the hardness across the interface, the Vickers microhardness measurements were made by a Vickers hardness tester (AKASHI JP/HM-122). Microstructures at the bonding interfaces were observed by an optical microscope (OM), stereo microscope, and scanning electron microscope (SEM). The chemical compositions were analyzed at the joint interface by an energy dispersive x-ray analysis (EDX).

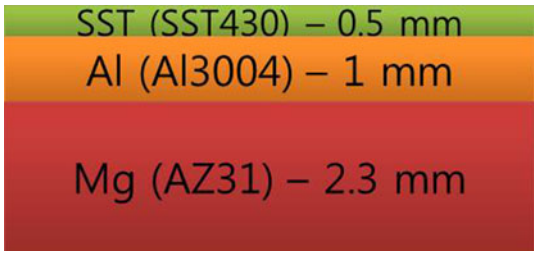

Fig. 1—Configuration and dimensions of AZ31Mg/3004 Al/SST 430 plates.

In order to precisely evaluate the contribution of each layer on the overall mechanical performance of the tri-layered Mg/Al/SST, each layer was separated from the clad Mg/Al/SST composite and mechanically tested independently to obtain the stress–strain curves. Separate Mg and SST sheets were obtained by dissolving the Al layer in NaOH solution for 24 hours at room temperature. Stainless steel is considered resistant to any concentration of sodium hydroxide below 353 K (80 °C).[13] Mg and its alloys were known to be stable in strong alkaline solutions such as NaOH solution because a layer of passive film would form on the surface which exhibits a good passive behavior.[14,15] Indeed, the surface of the separated SST plate in NaOH was found to be clean and a slight dark layer was observed on the separated Mg plate in NaOH, which appeared to act as a protective layer. After chemical separation, both Mg and SST were mechanically polished with care for mechanical testing. In order to exclude the effect of temperature-dependent intermetallic formation and its effect on the surface properties of separated sheets, each layer was annealed after separation. If Mg/Al/SST laminated plates were annealed at high temperatures [above 573 K (300 °C)] as they were bonded, the intermetallic layer forms especially at the Mg/Al interface, which would deteriorate the surface properties of separated Mg and Al sheets and reduce the thickness of Al and Mg sheets. The Al sheet was separated by mechanical polishing Mg and SST sheets away from the outer surface using a material polisher. All samples after mechanical polishing were observed to be clean and no visible defects were observed using a stereo microscope. The mechanical testing was repeated at least 3 times for each material's condition to insure that the results in this study are reliable, and the average strength values were used for the rule of mixture calculations.

III. RESULTS AND DISCUSSION

Figure 2 shows the optical micrographs of Al/SST interfaces for clad metals annealed at 473 K (200 °C) (a), 673 K (300 °C) (b), and 673 K (400 °C) (c) for

Table I. Chemical Compositions of Stainless Steel (SST 430), AL(Al 3004), and Mg(AZ31) Used in the Present Study (wt pct)

Material	Chemical Composition				
SST (SST 430)	Fe	Cr	Mn	Si	C
	79.8 to 84	≤0.18	≤1.0	≤1.0	≤0.12
Al (Al 3004)	Al	Mn	Mg	Fe	Si
	95.5 to 98.2	1 to 1.5	0.8 to 1.3	≤0.7	≤0.3
Mg (AZ 31)	Mg	Al	Zn	Mn	Si
	93.6 to 96.7	2.5 to 3.5	0.6 to 1.4	0.2 to 1	≤0.1

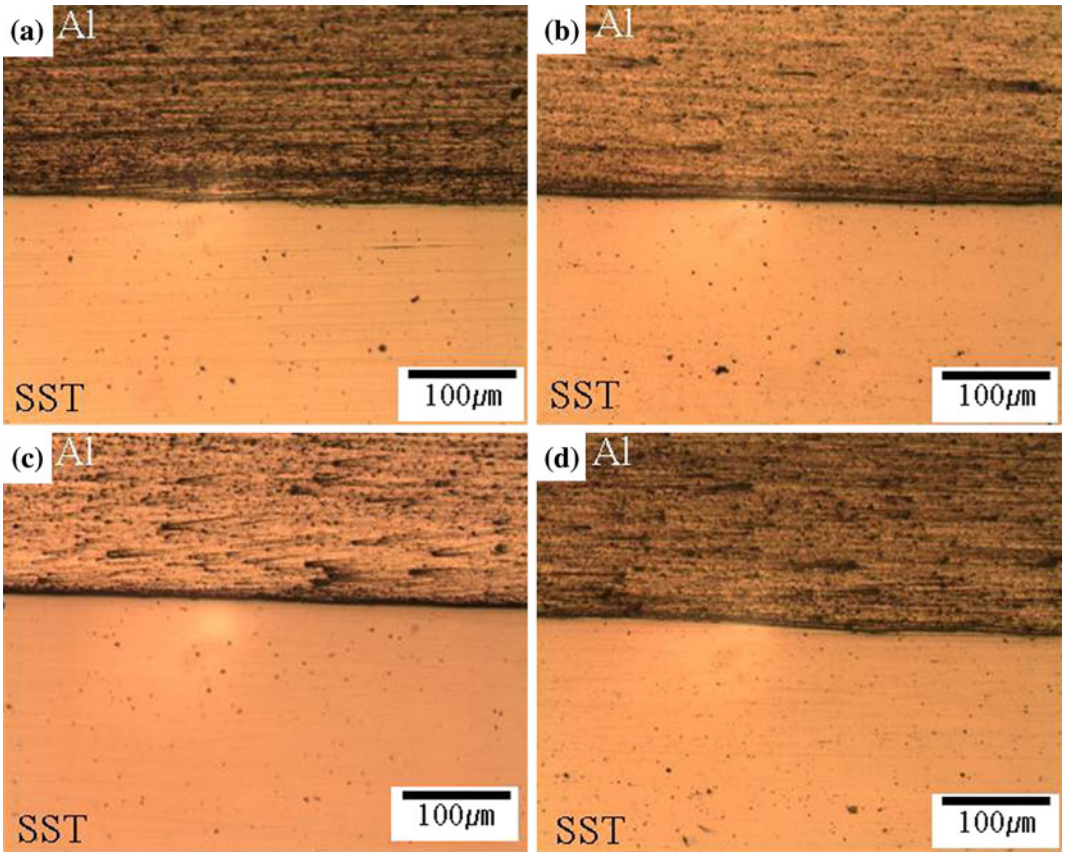

Fig. 2—Optical micrographs of Al/SST interface region in Mg/Al/SST clad metals, Mg/Al interface heat treated at 473 K (200 °C) for 1 h (*a*), 573 K (300 °C) for 1 h (*b*), 673 K (400 °C) for 1 h (*c*), and 673 K (400 °C) for 3 h (*d*).

1 hour and at 673 K (400 °C) for 3 hours (d). The Al/SST interface microstructure of the as-roll-bonded clad is similar to that of the clad annealed at 473 K (200 °C). No interfacial reaction layer was observed at the Al/SST interface using both optical microscopy and scanning electron microscopy (up to the magnification of ×2,500) in the as-rolled and all annealed clad metals. No interfacial cracks and flaws were observed, suggesting that the bonding interface between Al and SST is intact.[16–18] Figure 3 shows the optical micrographs of Mg/Al interfaces for clad metals annealed at 473 K (200 °C) (b), 573 K (300 °C) (c), and 673 K (400 °C) (d) for 1 hour and at 673 K (400 °C) for 3 hours (e). The interface region of the as-rolled clad plates is not shown in Figure 3 because the appearance of the interface of the as-rolled clad plates is similar to that of heat-treated clad plates at 473 K (200 °C). When the annealing temperature was at and above 573 K (300 °C), a reaction layer between Mg and Al was observed at Mg/Al interfaces as shown in Figures 3(b) through (d). The intermetallic layer at 573 K (300 °C) was found to be 12 μm thick. The thickness of the brittle intermetallic layer increased drastically at 673 K (400 °C) and it was measured to be approximately 56 and 96 μm after heat treatment for 1 and 3 hours, respectively.

Figure 4(a) shows the reaction compound layers between Al and Mg and the elemental distribution of Mg and Al from the intermetallic layers denoted by layer 1 (b) and layer 2 (c). It is shown that the reaction compound layer actually consisted of two layers with different Al and Mg compositions. The intermetallic compounds stable at room temperature in the Al–Mg system are Al_3Mg_2 and $Al_{12}Mg_{17}$ phases from the equilibrium phase diagram.[11] The ratio of Al to Mg peak intensity in the reaction compound layer adjacent to the Al layer is close to that of Al_3Mg_2[11] and the ratio in the reaction layer adjacent to the Mg layer is close to that of $Al_{12}Mg_{17}$. These reaction compounds are brittle and likely to deteriorate the bonding strength between the metallic layers. Figure 5 shows XRD peaks from the interface region of the clad composite annealed at 673 K (400 °C), which demonstrates the presence of Al_3Mg_2 and $Al_{12}Mg_{17}$. In Figure 4(a), the hardness of intermetallic layers measured by nanoindentation is also plotted. The hardness of Al_3Mg_2 (4.07 GPa) adjacent to Al was found to be greater than that of $Al_{12}Mg_{17}$ (3.76). Figure 6 displays the variation of intermetallic layer thickness with annealing condition. As shown in Figure 4, the thickness of Al_3Mg_2 is greater than that of $Al_{12}Mg_{17}$. For example, after heat treatment at 673 K (400 °C) for 3 hours, the thickness of Al_3Mg_2 and $Al_{12}Mg_{17}$ was found to be 68 and 28 μm, respectively.

In Figure 7, stress–strain responses of the as-roll-bonded clad plates and annealed clad plates at various temperatures are exhibited. One interesting observation is that the strain to the sudden drop of the flow stress

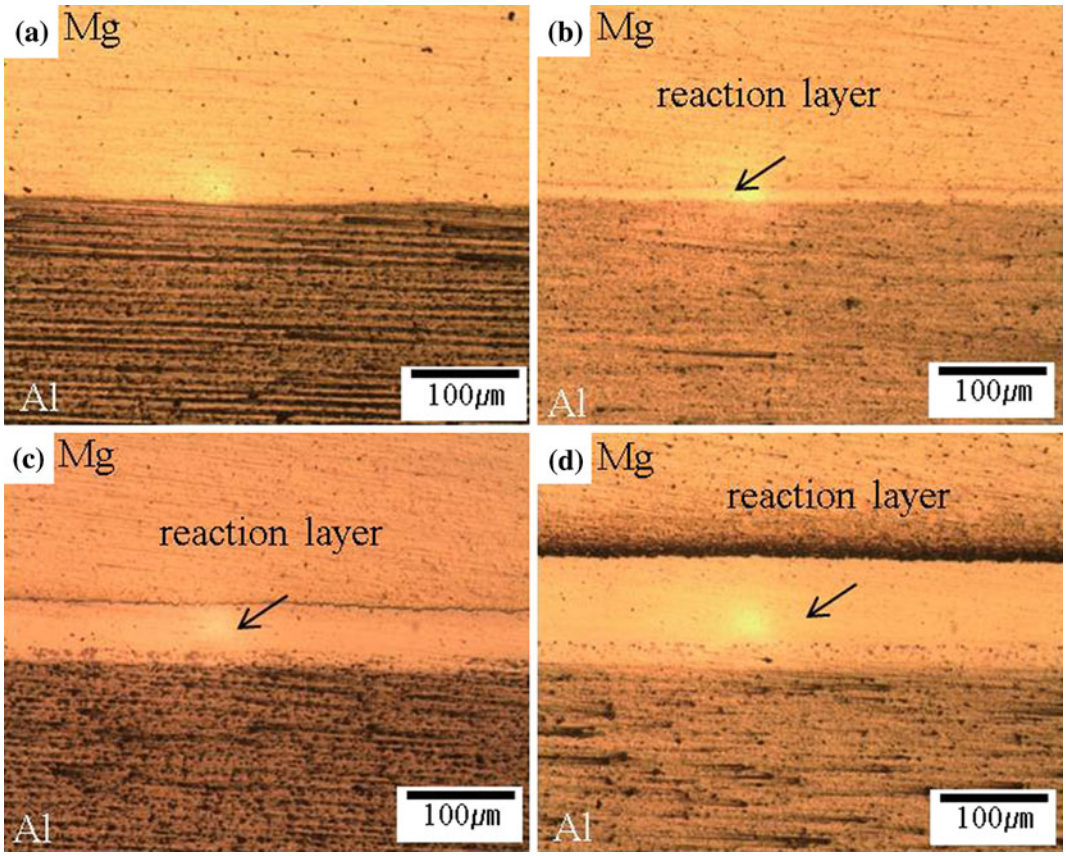

Fig. 3—Optical micrographs of Mg/Al interface region in Mg/Al/SST clad metals, Mg/Al interface heat treated at 473 K (200 °C) for 1 h (*a*), 573 K (300 °C) for 1 h (*b*), 673 K (400 °C) for 1 h (*c*), and 673 K (400 °C) for 3 h (*d*).

which is associated with the fracture of AZ31Mg[12] increased to ~24 pct total strain in the clad composite heat treated at 473 K (200 °C), but decreased to ~22 pct with increasing the heat treatment temperature to 573 K (300 °C). The fracture strain of the Mg layer further decreased from ~20 to 16.5 pct with increase of heat treatment time from 1 to 3 hours at 673 K (400 °C). The decrease of Mg fracture strain heat treated at 573 K and 673 K (300 °C and 400 °C) from that of the clad composite heat treated at 473 K (200 °C) is likely due to the presence of brittle intermetallic compound layers between the AZ31Mg alloy and the 3004 Al alloy. The reason for the significant increase of Mg layer fracture strain after heat treating at 473 K (200 °C) is not clear, which may be due to the increase of the Mg/Al interfacial bonding strength or the simple increase of Mg fracture strain itself with heat treatment at 473 K (200 °C). The concurrent fracture of 3004 Al and SST 430 supports the excellent bonding between these two alloys. As shown in Figure 2, no reaction compounds were observed at the Al/SST interfaces in the as-rolled and heat-treated clad plates, which may have contributed to the concurrent fracture of Al and SST. In Figure 7, three stress components, σ_y, σ_F, and $\sigma_{Al/SST}$, and strain components, ε_F, ε_{Mg}, and ε_R ($=\varepsilon_F - \varepsilon_{Mg}$), are marked on the stress–strain curve of the as-roll-bonded plate for illustrative purposes. The stress components σ_y, σ_F, and $\sigma_{Al/SST}$ are the yield strength of Mg/Al/SST clad plates, the strength just before the Mg alloy fracture, and the strength just after Mg alloy fracture, respectively, and the strain components, ε_F, ε_{Mg}, and ε_R ($=\varepsilon_F - \varepsilon_{Mg}$) are the total fracture strain, the strain to fracture of AZ31Mg alloy layer (the strain to the first load drop), and the remaining strain component after fracture of the AZ31Mg alloy layer, ε_R ($=\varepsilon_F - \varepsilon_{Mg}$), respectively. These stress and strain components can be obtained from the stress–strain curves of heat-treated clad composites (Figure 7) to analyze the contribution of each layer to the mechanical performance of clad as will be discussed with reference to Figures 9 and 10.

Figures 8(a) through (c) display the stress–strain responses of Mg sheet, Al sheet, and SST sheet, respectively, which were separated from the as-roll-bonded and annealed clad composite plates. One noticeable observation from stress–strain responses is that the fracture strain of the separated Mg sheet increased drastically and the flow stress decreased appreciably with heat treatments of 473 K to 673 K (200 °C to 400 °C). The stress–strain responses of separated Mg from the as-roll-bonded clad composite and that annealed at 473 K (200 °C) are quite similar to the initial parts of stress–strain responses of the whole Mg/Al/SST clad, suggesting that the increase of the strain to the first load drop after annealing at 473 K (200 °C) is mainly caused by the ductility increase of Mg itself. Figure 8(b) demonstrates that the fracture strain

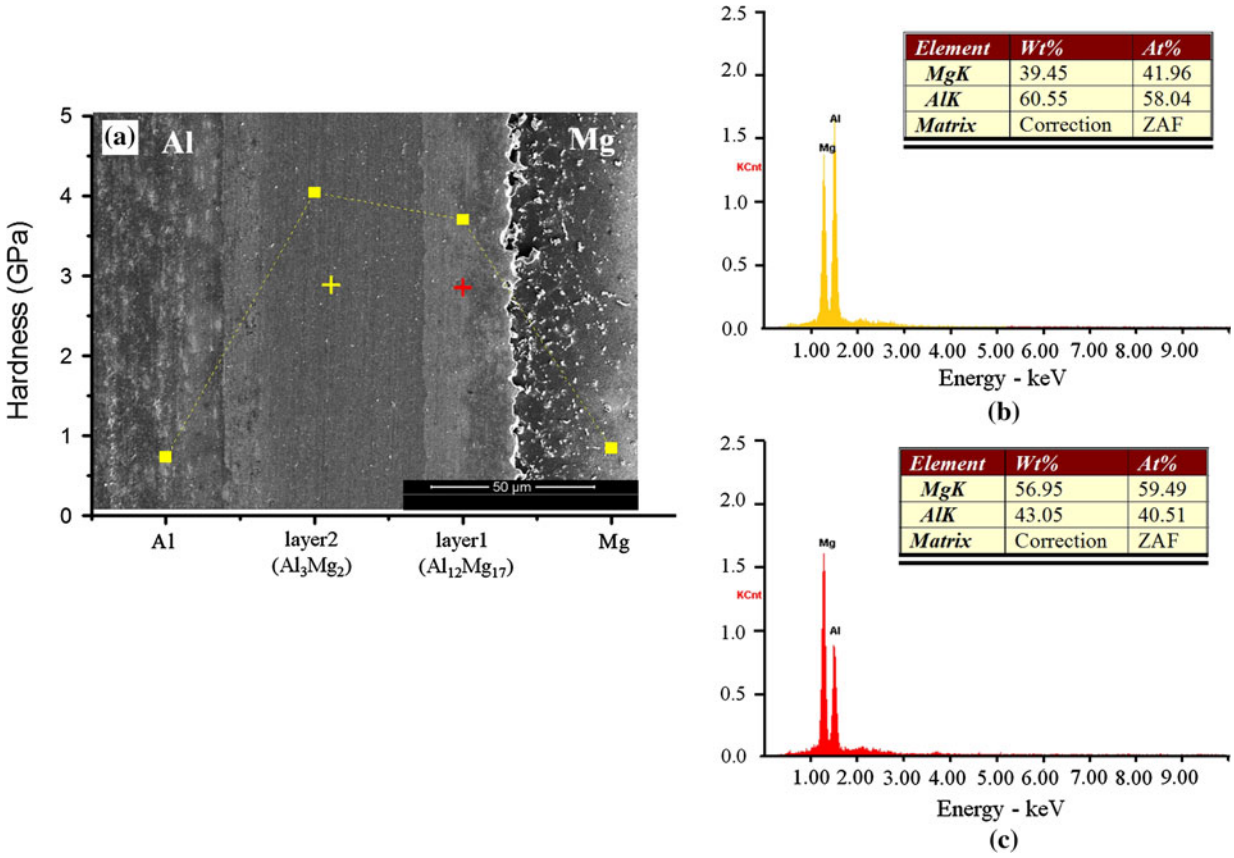

Fig. 4—(*a*) Interfacial reaction compound layer between Al and Mg, (*b*) EDS spectra from the interfacial compound layer adjacent to Al, (*c*) EDS spectra from the interfacial compound layer adjacent to Mg (the peaks were obtained from the point indicated by a cross mark).

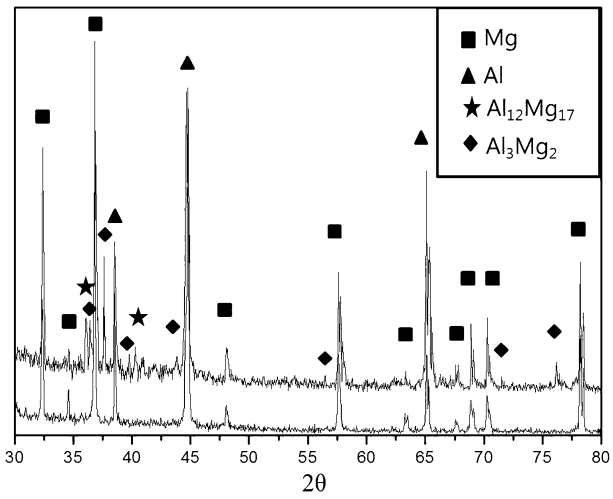

Fig. 5—XRD peaks from the interface region of the clad composite annealed at 400 K, which demonstrates the presence of A_3Mg_2 and $Al_{12}Mg_{17}$.

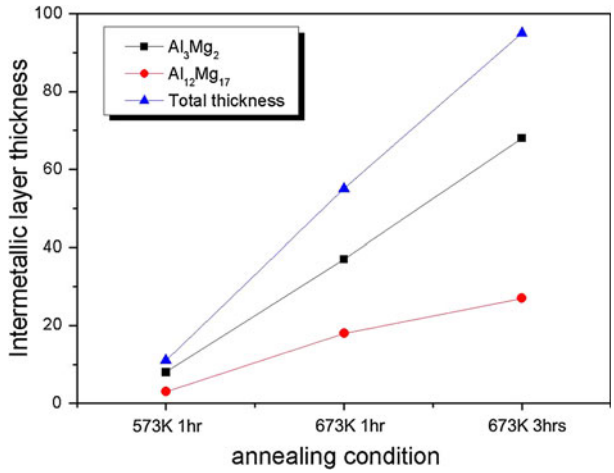

Fig. 6—Thickness of intermetallic layers varied with annealing condition.

of separated Al increased gradually from 573 K (300 °C) and reached 35 pct total fracture strain after heat treating at 673 K (400 °C). The increase of fracture strain of separated Mg and Al layers is due to the recovery/recrystallization of these metals. The fracture strain of Mg increased more rapidly at lower temperatures because it has the lower recrystallization temperature. Stress–strain responses of the separated SST sheet also show that the fracture strain also increased after heat treatments at 473 K to 673 K (200 °C to 400 °C) without any appreciable change of the flow stress.

Figure 9 exhibits the stress components obtained by analyzing the strain–strain responses of the tri-layered

Mg/Al/SST clad plates shown in Figure 7. In this figure, the yield strength of the Mg/Al/SST clad plates σ_y, the strength just before the Mg alloy fracture σ_F, and the strength just after Mg alloy fracture $\sigma_{Al/SST}$ are plotted. The stress components from the mechanical data of the tri-layered Mg/Al/SST are indicated by closed symbols and dashed lines in Figure 9. The decreases of the yield strength of clad plates σ_y and the strength just before Mg fracture with annealing temperature can be attributed to the softening associated with recovery/recrystallization. It is noted that the strength just after Mg fracture $\sigma_{Al/SST}$ for Mg/Al/SST clad plates (114~101 MPa) did not change much with annealing temperature, reflecting the insensitivity of the flow stress of SST to annealing up to 673 K (400 °C) and the absence of a brittle intermetallic layer between SST and Al. In Figure 9, the thickness-compensated average yield strength and strength just before Mg fracture calculated based on the yield stress and ultimate tensile strength data of the separated Mg, Al, and SST sheets by taking the thickness fractions of Mg, Al, and SST of clad into consideration were also plotted for comparison with the strength data of the tri-layered Mg/Al/SST clad. As shown in Figure 9, the yield strength and UTS (indicated by closed symbols, dashed lines) of the tri-layered Mg/Al/SST clad plates are in close agreement

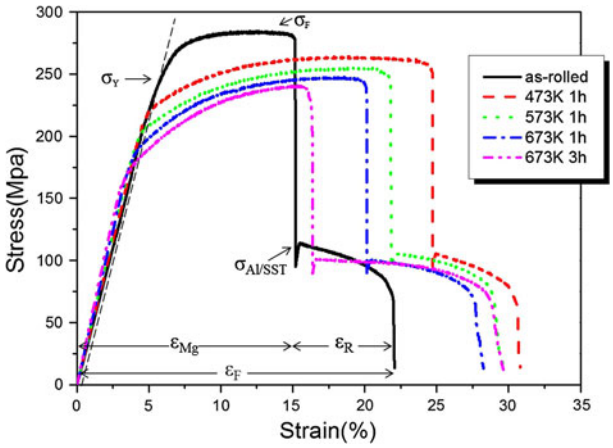

Fig. 7—Stress–strain responses of as-roll-bonded clad plates and annealed clad plates at various temperatures.

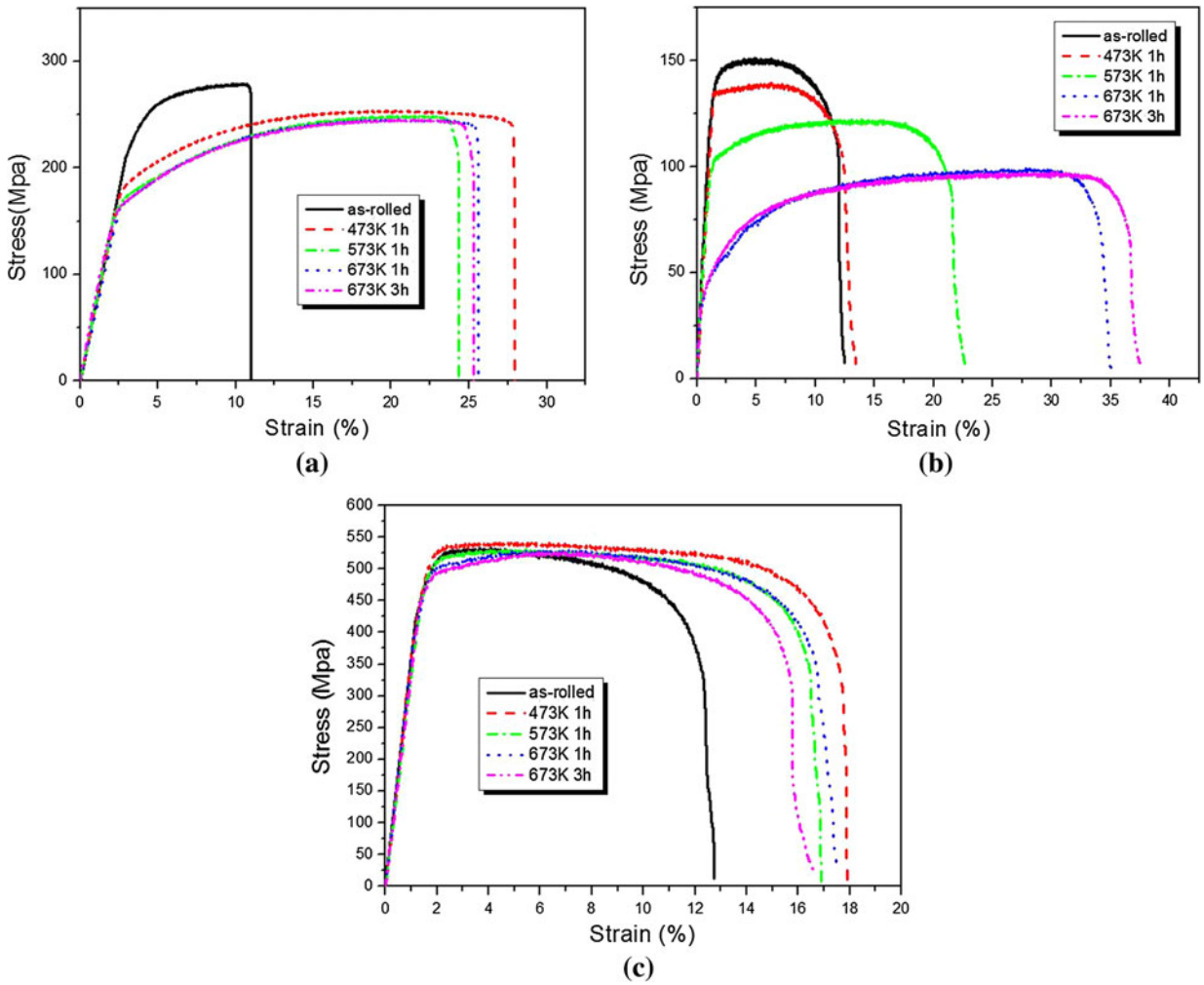

Fig. 8—Stress–strain responses of independent Mg sheet (*a*), Al sheet (*b*), and SST sheet (*c*), which were separated from as-roll-bonded and annealed clad composite plates.

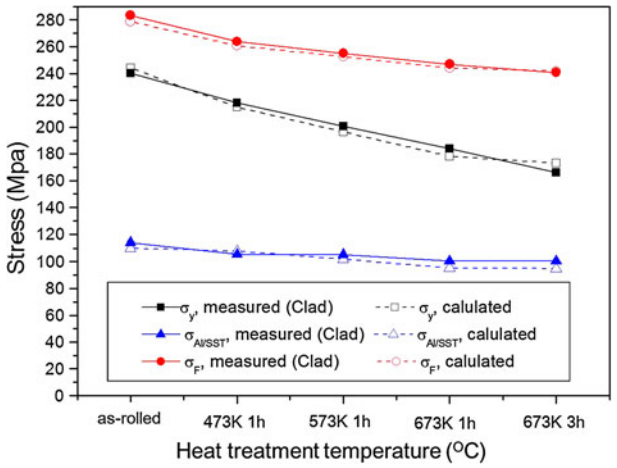

Fig. 9—Stress components obtained by analyzing the strain–strain responses of tri-layered Mg/Al/SST clad plates. The yield strength of Mg/Al/SST clad plates, σ_y, the strength just before Mg alloy fracture σ_F, the strength just after Mg alloy fracture $\sigma_{Al/SST}$, and the strength contribution from Mg alloy layer σ_{Mg} ($\sigma_F - \sigma_{Al/SST}$) are plotted as a function of heat treatment temperature.

with those (indicated by open symbols, dotted lines) calculated from the strength data of the separated Mg, Al, and SST layers, suggesting the strength of the tri-layered composites obeys the rule of mixture. The strength of the tri-layered clad was also found to agree well with the thickness-compensated average strength of the separated Al and SST, suggesting the mechanical stability of the Al/SST plate even after the catastrophic Mg fracture. In Table II, the stress components of the clad composite plate and the separated Al, Mg, and SST sheets are summarized in comparison with the calculated strength values obtained by the rule of mixture. The strength of the Mg/Al/SST laminated plate is close to that of Mg (AZ31) because the strength increase by SST is compensated by the decrease of strength due to the soft Al layer as shown in Figures 7 and 8(a). There appears to be no obvious benefit of using Mg/Al/SST clad plates in terms of mechanical properties. But, the major benefit of cladding Mg with SST is to exploit the excellent corrosion resistance of stainless steels at the reduced density.

Figure 10 exhibits the strain components obtained by analyzing the strain–strain responses of the clad plates shown in Figure 7. In Figure 10, the total fracture strain ε_F, the strain to fracture of the AZ31Mg alloy layer (the strain to the first load drop) ε_{Mg}, and the remaining strain component after fracture of the AZ31Mg alloy layer, ε_R ($=\varepsilon_F - \varepsilon_{Mg}$) were plotted (closed symbols, dashed lines). The strain components from the mechanical data of tri-layered Mg/Al/SST are indicated by closed symbols and dashed lines in Figure 10. The total fracture strain increased appreciably after heat treating at 473 K (200 °C) and then decreased gradually with increasing heat treatment temperature above 473 K (200 °C). With increase of annealing time at 673 K (400 °C), a slight increase of total fracture strain was observed. It is also clear from Figure 10 that the fracture strain of the Mg layer (the strain to first load drop) also

Table II. Experimental Strength Values in Comparison with those of the Rule of Mixture

	Experimental								Rule of Mixture	
	Clad			Mg		Al		SST	$\sigma_{MG}f_{MG}+\sigma_{AL}f_{AL}+\sigma_{SST}f_{SST}$	$\sigma_{AL}f_{AL}+\sigma_{SST}f_{SST}$
Processing	σ_Y	σ_F	σ_{AlSST}	σ_Y	σ_F	σ_Y	σ_F	σ_Y	σ_F	σ_Y	σ_F
As-rolled	240.3	283.4	114.1	233.5	279.0	140.8	151.2	514.4	532.5	246.1	278.7	109.8
473 K 1 h	218.1	263.8	105.5	181.5	253.5	135.0	139.4	527.8	541.9	214.9	261.4	107.9
573 K 1 h	200.6	255.0	105.3	168.6	248.9	103.3	122.1	508.7	530.6	196.1	252.6	101.9
673 K 1 h	184.0	246.9	100.4	166.6	244.7	43.4	99.1	498.3	530.2	177.9	244.0	95.8
673 K 3 h	166.2	240.8	100.5	163.0	243.0	42.6	96.8	489.1	526.5	174.2	241.8	94.7

Unit: MPa.

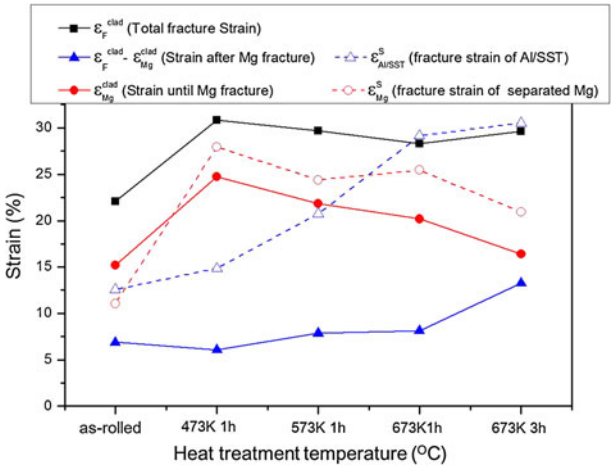

Fig. 10—Strain components obtained by analyzing the strain–strain responses of clad plates. The total fracture strain ε_F, the strain to fracture of AZ31Mg alloy layer (the strain to the first load drop) ε_{Mg}, and the remaining strain component after fracture of AZ31Mg alloy layer ε_R ($=\varepsilon_F - \varepsilon_{Mg}$) are plotted as a function of heat treatment temperature.

increased after heat treating at 473 K (200 °C) and gradually decreased above 473 K (200 °C). It is interesting to note that the remaining strain after Mg alloy fracture, which is the strain to the final failure after Mg alloy fracture, increased with increasing the heat treatment temperature despite the decreasing fracture strain of AZ31Mg alloy layer. This means that the fracture strain of the joined Al/SST430 plate increases with increasing heat treatment temperature and time, which may be caused by the drastic increase of fracture strain of Al with increase of heat treatment temperature.

In Figure 10, the fracture strains of the separated Mg and the average fracture strain of separated Al and SST (indicated by open symbols, dotted lines) are also plotted for comparison with the fracture strain components of the tri-layered Mg/Al/SST clad composites (indicated by closed symbols, dashed lines). The fracture strain of the separated Mg sheet increased significantly after heat treating at 473 K (200 °C) and slightly decreased with heat treatment at higher temperatures. The strain until Mg fracture in the tri-layered Mg/Al/SST clad follows a similar trend as the fracture strain of separated Mg sheets, but the Mg fracture strains in the Mg/Al/SST clad were found to be generally smaller than those of separated Mg sheets after heat treatments above 473 K (200 °C). Therefore, the decrease of total fracture strain after heat treating at high temperatures is caused by the reduction of Mg alloy fracture strain. The reduction of Mg fracture strain after annealing at high temperatures is most likely linked to brittle fracture of a reaction compound layer adjacent to the AZ31Mg alloy layer. One of the most interesting observations is that the total fracture strain of the tri-layered Mg/Al/SST clad was found to be higher than the thickness-compensated average fracture strain calculated from the fracture strain data of the separated Mg, Al, and SST sheets by taking the thickness fractions of Mg, Al, and SST of clad into consideration. Unlike the excellent agreement between the stress components of the tri-layered clad and those calculated based the strength data of separated Mg, Al, and SST sheets, the fracture strain components of the tri-layered clad far exceed those calculated based the fracture strain data of separated Mg, Al, and SST sheets. It is interesting to note that the total fracture strain of the tri-layered Mg/Al/SST clad after heat treatment at 673 K (400 °C) is quite close to the calculated thickness-compensated average fracture strain of Al and SST. It was found that the thickness of the brittle intermetallic layer increased drastically over 70~120 μm at 673 K (400 °C). The presence of thick brittle layers between Mg and Al may have allowed the Mg layer and the rest of the Al/SST layer to behave almost independently because of early fracture of intermetallic layer during tensile testing. In this case, the total fracture strain can be determined by the co-fracture of Al and SST independent of premature Mg fracture, which was found to be joined concretely until the final fracture.

Figure 11 shows the stereo microscopic images of the lateral surface showing the SST/Al interface parallel to the stress axis of Mg/Al/SST clad plates heat treated at 473 K (200 °C) for 1 hour (25 pct strain) (a), at 573 K (300 °C) for 1 hour (20 pct strain) (b), at 673 K (400 °C) for 1 hour (20 pct strain) (c), and 3 hours (15 pct strain) (d) just before Mg fracture (*i.e.,* just before the first load drop). A lateral surface image of as-roll-bonded Mg/Al/SST is not shown here because it does not show any distinctive features. Since tests were stopped just before Mg fracture, the total applied strain differs from test to test. The Al side appears to deform uniformly and no slip lines and bands were observed, suggesting uniform and fine slip which may be associated with the high stacking fault energy.[18,20] In the SST side, the surface appears bumpy because of the slip asymmetry in each grain, which makes the grain morphology and grain boundaries more clearly defined and visible. It is well known that asymmetric slip in the BCC structure promotes the shape change of crystals and grains.[21–23] The slip traces in the grains were also clearly visible in SST.

One important thing to be noted is that SST does not show any indication of cracks and fracture even after 15 to 25 pct strain despite the low fracture strain (12 to 18 pct) of the separated independent SST sheet. For example, SST in the tri-layered Mg/Al/SST clad heat treated at 573 K (300 °C) displayed in Figure 10(b) was deformed to 20 pct total strain without any indication of fracture, although the fracture strain of the independent SST layer separated from the same clad specimen heat treated at the same temperature was 17 pct as shown in Figure 8(c). Actually, the SST/Al joined layer in the Mg/Al/SST clad heat treated at 573 K (300 °C) fractured at the total strain of 28 pct, which is far greater than the fracture strain (~17 pct) of the separated SST sheet as shown in Figures 7 and 10. Hong and Laird[19,20] suggested that the homogeneous slip of each grain in the B.C.C. metals promoted the development of bumpy surface along grain boundaries due to the mismatch of accumulated deformation at grain boundaries. Therefore, the presence of bumpy surface in the SST side along the long interface suggests the overall homogeneous

deformation in SST of the tri-layered Mg/Al/SST clad composite, resulting in the enhanced ductility of the SST sheet deformed in the Mg/Al/SST clad.

Figure 12 shows the stereo microscopic images of the lateral surface showing the Mg/Al interface parallel to the stress axis of the Mg/Al/SST clad plates heat treated at 473 K (200 °C) for 1 hour (25 pct strain) (a), at 573 K (300 °C) for 1 hour (20 pct strain) (b), at 673 K (400 °C) for 1 hour (20 pct strain) (c), and 3 hours (15 pct strain) (d) just before Mg fracture (*i.e.*, just before the first load drop). Lateral surface image of as-roll-bonded Mg/Al/SST is not shown in this figure. Again, the Al side appears to deform uniformly and no slip lines and bands were observed because of uniform and fine slip in Al with high stacking fault energy.[19] In the Mg side, the surface exhibited the orange peel-like appearance, suggesting the grain size is relatively small and the overall deformation is homogeneous even at the total strain of 25 pct in the Mg/Al/SST clad heat treated at 473 K (200 °C) (a). No interfacial cracks were observed. The clad heat treatment at 573 K (300 °C) (b) exhibited the short horizontal cracks perpendicular

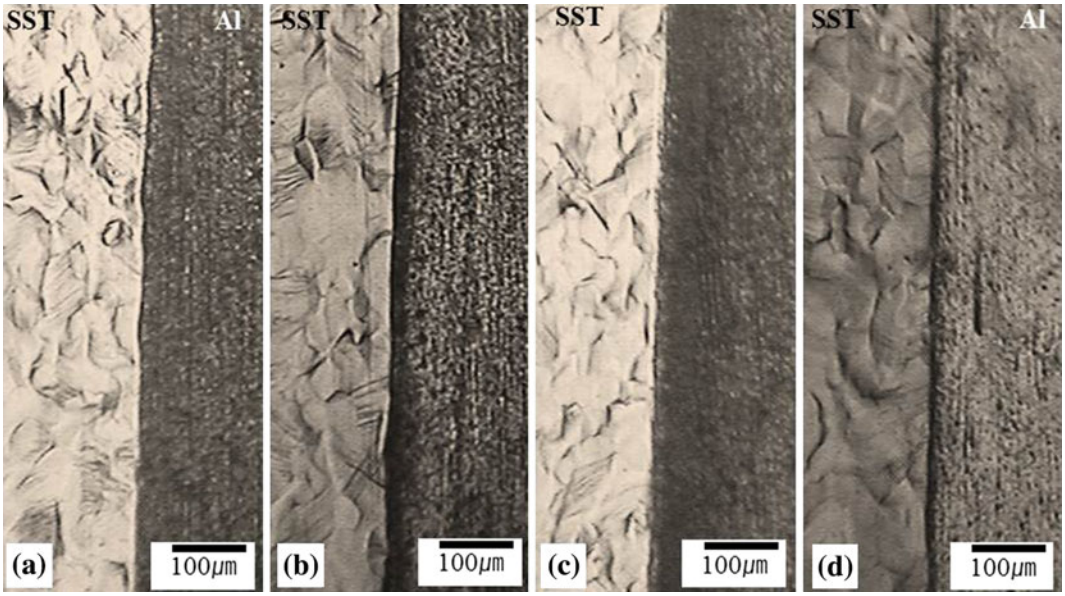

Fig. 11—Stereo microscopic images of the lateral surface showing the SST/Al interface parallel to the stress axis of Mg/Al/SST clad plates heat treated at 473 K (200 °C) for 1 h (25 pct strain) (*a*), at 573 K (300 °C) for 1 h (20 pct strain) (*b*), at 673 K (400 °C) for 1 h (20 pct strain) (*c*), and 3 h (15 pct strain) (*d*) just before Mg fracture (*i.e.,* just before the first load drop).

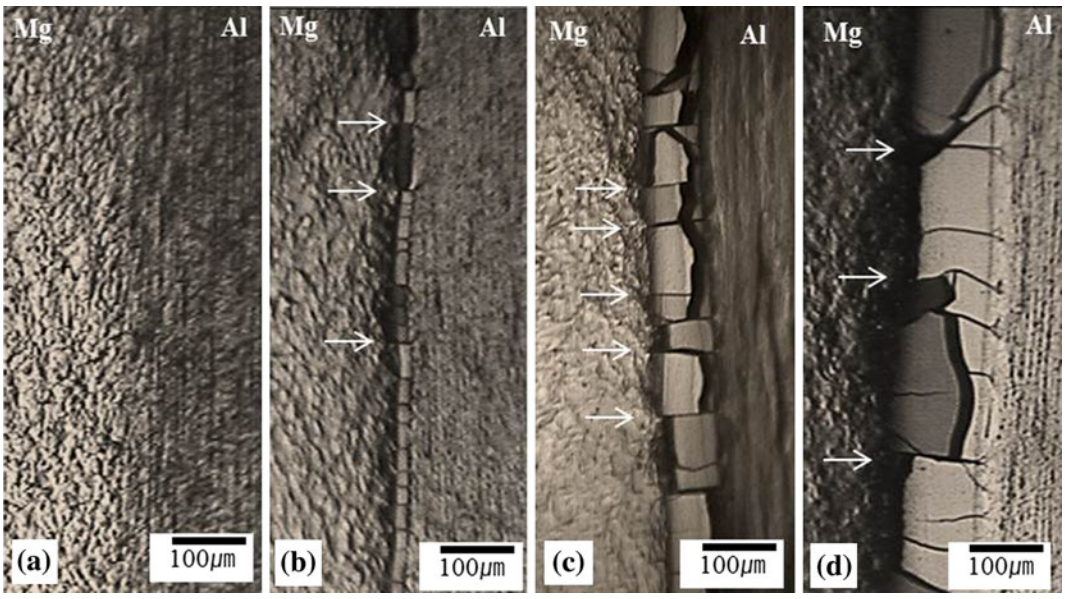

Fig. 12—Stereo microscopic images of the lateral surface showing the Mg/Al interface parallel to the stress axis of Mg/Al/SST clad plates heat treated at 473 K (200 °C) for 1 h (25 pct strain) (*a*), at 573 K (300 °C) for 1 h(20 pct strain) (*b*), at 673 K (400 °C) for 1 h (20 pct strain) (*c*), and 3 h (15 pct strain) (*d*) just before Mg fracture (*i.e.*, just before the first load drop).

to the interface; in the interfacial intermetallic layer, the Mg substrate close to the interface displayed the evidence of localized deformation especially close to the cracks.

The clad heat treatment at 673 K (400 °C) for 1 hour (c) and 3 hours (d) exhibited not only the horizontal cracks but also the vertical cracks in the interfacial intermetallic layer. The Mg substrate close to the interface displayed the evidence of localized deformation.(as marked by arrows) especially close to the cracks. The cracks are likely developed in the stress-concentrated region in the vicinity of horizontal cracks in the intermetallic layer. It should be noted that the number of cracks decreased as the thickness of the intermetallic layer increased with increasing the heat treatment time from 1 to 3 hours at 673 K (400 °C). The interval between the horizontal cracks increased with increasing the thickness of the intermetallic layer since the horizontal cracks are formed when the shear stress on the interface during tension is high enough to induce normal fracture stress of the intermetallic layer. Figure 13 shows the inter-horizontal crack spacing versus the intermetallic layer thickness.

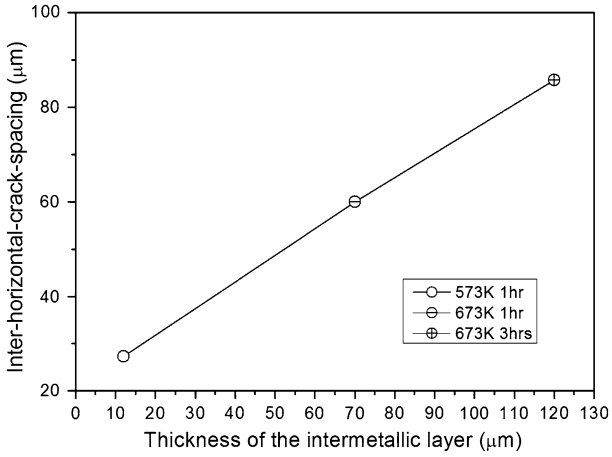

Fig. 13—Inter-horizontal crack spacing plotted against the intermetallic layer thickness.

Figure 14 shows the consecutive stereo microscopic images of the lateral surface showing the Mg/Al interface parallel to the stress axis of the Mg/Al/SST clad plates heat treated at 673 K (400 °C) for 1 hour as a function of total strain. Figure 14(a) exhibits the Al/Mg interface region of specimens strained to 5 pct (a), 10 pct (b), 15 pct (c), and 20 pct (d). Cracks perpendicular to the stress axis were observed in the intermetallic layer at 5 pct strain as shown in Figure 8(a). The number of cracks apparently increased after the specimen deformed to 10 pct strain. These cracks were formed because of the strain mismatch between metal layers and the reaction compound layer. It should be noted that strain-concentrated slip lines (marked with arrows) developed in the localized region of the Mg alloy layer in the vicinity of the cracks. This slip localization intensified with increasing strain as shown in Figures 14(c) and (d). It seems obvious that this slip localization in the vicinity of cracks in the intermetallic layer induced premature cracking of Mg alloy, resulting in the decreased Mg fracture strain (Figures 5 and 6) with increasing heat treatment temperature.

One interesting and important observation in this study is that the well-bonded clad metals exhibited more enhanced ductility than the separated independent single layer of metal. It is postulated that the enhanced ductility of constituent metals in the well-bonded clad compared to the separated independent metal layer is caused by the suppression of the localized deformation in a metallic layer by other metallic layers. If the strain

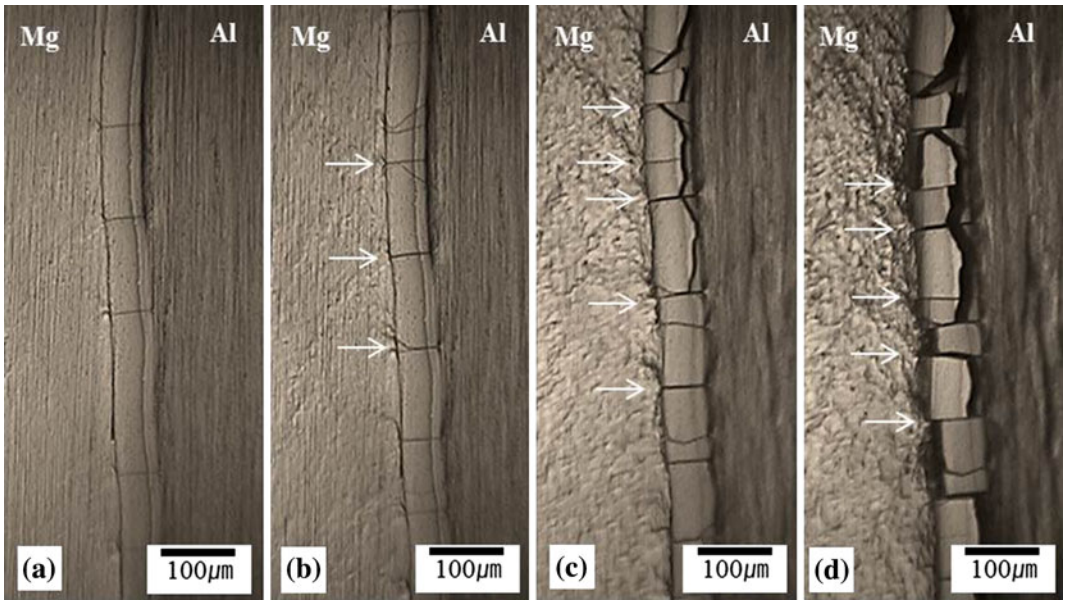

Fig. 14—Consecutive stereo microscopic images of the lateral surface showing the Mg/Al interface parallel to the stress axis of Mg/Al/SST clad plates heat treated at 673 K (400 °C) for 1 h as a function of total strain. Specimens strained to 5 pct (*a*), 10 pct (*b*), 15 pct (*c*), and 20 pct (*d*).

localization develops in a single layer of metals, the localization is intensified if there is no significant work hardening. On the other hand, further intensification of localization is hindered by other metallic layers if these layers are well bonded in the layered clad metals, leading to the enhanced ductility. If the bonding becomes weak by the formation of brittle intermetallic layers, the positive effect on the ductility enhancement in the clad does not work. In this study, the ductility enhancement was observed in the well-bonded clad plates. It was also observed that the ductility decreased if the interface was weak by the formation of the intermetallic layer, and the cracks in the intermetallic layer affect the adjacent metallic layer.

IV. SUMMARY

The mechanical responses and fracture behaviors of the as-rolled and heat-treated Mg/Al/SST clad composite plates were studied and are summarized as follows:

1. No interfacial reaction layer and flaws were observed at the Al/SST interface in the as-rolled and annealed clad metals, suggesting the bonding interface between Al and SST is intact. An interfacial compound layer was observed at the Mg/Al interface after annealing at and above 573 K (300 °C). The presence of Al_3Mg_2 and $Al_{12}Mg_{17}$ at the Al/Mg interface was confirmed by XRD.
2. The yield strength and UTS of the tri-layered Mg/Al/SST clad plates are in close agreement with those calculated from the strength data of the separated Mg, Al, and SST layers, suggesting the strength of the tri-layered composites obeys the rule of mixture.
3. The total fracture strain of the Mg layer increased appreciably after heat treating at 473 K (200 °C) and then decreased gradually with increasing heat treatment temperature. The significant increase of the Mg layer fracture strain in the Mg/Al/SST after heat treating at 473 K (200 °C) was found to be mainly due to the increase of Mg fracture strain itself at 473 K (200 °C). The decrease of Mg fracture strain heat treated at 573 K and 673 K (300 °C and 400 °C) is due to the presence of brittle reaction compound layers between the AZ31Mg alloy and 3004 Al.
4. Cracks perpendicular to the stress axis were observed in the reaction compound layer at 5 pct strain in the clad plates heat treated at 673 K (400 °C). The number of cracks increased with increase of strain and the number of cracks decreased with increase of intermetallic layer thickness. The strain-concentrated slip lines developed in the Mg alloy layer in the vicinity of intermetallic cracks and intensified with increasing strain, inducing premature cracking of the Mg layer.
5. The total fracture strain of the tri-layered Mg/Al/SST clad was found to be higher than the thickness-compensated average fracture strain calculated from the fracture strain data of the separated Mg, Al, and SST sheets. The localized deformation in one layer of metals is hindered by the mutual constraint imposed by adjacent layer if these layers are well bonded, leading to the enhanced ductility.

ACKNOWLEDGMENTS

This work was supported by a grant from the Fundamental R & D Program for Core Technology for Materials (2010) funded by the Ministry of Knowledge Economy.

REFERENCES

1. R.C. Zeng, W. Ke, Y.B. Xu, E.H. Han, and Z.G. Zhu: *Acta Metall Sin.*, 2001, vol. 37, pp. 673–85.
2. R.E. Brown: *Light Metal Age*, 2001, vol. 59, pp. 54–56.
3. S.F. Su, J.C. Huang, H.K. Lin, and N.J. Ho: *Metall. Mater. Trans. A*, 2002, vol. 33A, pp. 1461–73.
4. G.S. Cole and A.M. Sherman: *Mater. Charact.*, 1995, vol. 35, pp. 3–9.
5. Y. Kojima: *Mater. Trans.*, 2001, vol. 42, pp. 1154–59.
6. H. Haferkamp, R. Boehm, U. Holzkamp, C. Jaschick, V. Kaese, and M. Niemeyer: *Mater. Trans.*, 2001, vol. 42, pp. 1160–66.
7. H. Matsumoto, S. Watanabe, and S. Hanada: *J. Mater. Proc. Technol.*, 2005, vol. 169, pp. 9–15.
8. A. Çetin, J. Krebs, A. Durussel, A. Rossoll, J. Inoue, T. Koseki, S. Nambu, and A. Mortensen: *Metall. Mater. Trans. A*, 2011, vol. 42A, pp. 3509–20.
9. H. Takuda and N. Hatta: *Metall. Mater. Trans. A*, 1998, vol. 29A, pp. 2829–34.
10. K. Yilamu, R. Hino, H. Hamasaki, and F. Yoshida: *J. Mater. Process. Technol.*, 2010, vol. 210, pp. 272–78.
11. S. Brennan, K. Bermudez, N.S. Kulkarni, and Y. Sohn: *Metall. Mater. Trans. A*, 2012, vol. 43A, pp. 4043–52.
12. I.K. Kim, J.Y. Song, Y.S. Lee, and S.I. Hong: *Kor. J. Met. Mater.*, 2011, vol. 49, pp. 664–71.
13. F.L. LaQue and H.R. Copson: *Corrosion Resistance of Metals and Alloys*, 2nd ed., ACS monographs 158, Reinhold Publishing Corp., 1963, p. 410.
14. J. Chen, J. Wang, E.-H. Han, and W. Ke: *Corros. Sci.*, 2009, vol. 51, pp. 477–84.
15. S.J. Kim, M. Okido, Y. Mizutani, R. Ichino, S. Trnikawa, and S. Hasegawa: *Mater. Trans.*, 2003, vol. 44, pp. 1036–41.
16. X.J. Sun, J. Tao, and X.Z. Guo: *Trans. Nonferrous Met. Soc. China*, 2011, vol. 21, pp. 2175–80.
17. D.H. Bae, S.J. Jung, Y.R. Cho, W.S. Jung, H.S. Jung, C.Y. Kang, and D.S. Bae: *Kor. J. Met. Mater.*, 2009, vol. 47, pp. 573–80.
18. S.I. Hong and J.S. Song: *Metall. Mater. Trans. A*, 2001, vol. 32A, pp. 985–91.
19. S.I. Hong and C. Laird: *Acta Metall. Mater.*, 1990, vol. 38, pp. 1581–94.
20. S.I. Hong and C. Laird: *Mater. Sci. Eng.*, 1989, vol. A110, pp. L23–L26.
21. H. Mughrabi, K. Herz, and X. Stark: *Int. J. Fract.*, 1981, vol. 17, pp. 193–220.
22. H.D. Manesh and A.K. Taheri: *J. Alloys Comp.*, 2003, vol. 361, pp. 138–43.
23. M. Anglada: *Phys. Status Solidi (a)*, 1980, vol. 62, pp. 197–206.